Letter

Nonlinear kinetic estimate of Raman reflectivity in a hohlraum plasma with a radiation hydrodynamics code

D. Bénisti [1,2,*] O. Morice [1] C. Rousseaux [1] A. Debayle,[1,2] P. E. Masson-Laborde [1,2] and P. Loiseau [1,2]

[1]*CEA, DAM, DIF, F-91297 Arpajon, France*
[2]*Université Paris-Saclay, CEA, LMCE, F-91680 Bruyères-le-Châtel, France*

In this Letter, we introduce an inline model for stimulated Raman scattering (SRS), which runs on our radiation hydrodynamics code TROLL. This model accounts for nonlinear kinetic effects and for the SRS feedback on the plasma hydrodynamics. We dubbed it PIEM because it is a fully "PredIctivE Model," because no free parameter is to be adjusted *a posteriori* in order to match the experimental results. PIEM predictions are compared against experimental measurements performed at the Ligne d'Intégration Laser. From these comparisons, we discuss the PIEM ability to correctly catch the impact of nonlinear kinetic effects on SRS.

Introduction. An effective modeling of nonlinear kinetic effects, able to address large-scale systems, has been a long-standing issue relevant to many fields of physics. These include laser-plasma interactions, and in particular stimulated Raman scattering (SRS) [1], which we focus on in this Letter. SRS is a serious threat for laser fusion, as clearly demonstrated by the first experiments at the National Ignition Facility (NIF) [2]. This was one motivation to introduce a new design, with a low gas fill and shorter pulse duration, which successfully led to ignition [3]. However, there is still no way to make predictive simulations as regards laser-plasma interaction on such facilities as the NIF, or the Laser Mégajoule, that would help introduce new and maybe more effective designs.

In order to accurately predict Raman reflectivity, one would usually need a code that correctly estimates nonlinear kinetic effects. However, only a rad-hydro code can address the space scales and timescales relevant to inertial confinement fusion (ICF) experiments. This calls for an inline model (i.e., which runs directly on a rad-hydro code), able to derive Raman reflectivity by accounting for nonlinear kinetic effects. Yet, we are only aware of very few published inline models for SRS. Stark *et al.* derived in Ref. [4] a semiempirical model based on a parameter study with two-dimensional particle-in-cell simulations, in essentially uniform plasmas. This model was designed to run on a rad-hydro code but has not yet been implemented in such a code. In Ref. [5], Colaïtis *et al.* introduced a scaling law in the rad-hydro code CHIC in order to estimate the temperature of energetic electrons produced by SRS. In Ref. [6], Strozzi *et al.* introduced a linear kinetic modeling of SRS in the rad-hydro code LASNEX. However, this was a *post hoc* model which required experimental data.

In this Letter, we introduce a predictive model (dubbed PIEM) which predicts the SRS reflected power and wavelengths without needing any input from experimental measurements. It has been implemented in our rad-hydro code TROLL [7] and allows for the SRS feedback on the plasma hydrodynamics. It is derived from a rigorous theory [8–10] after several simplifying assumptions and, as shown in Fig. 3, its predictions compare well with experimental measurements. The latter measurements were not obtained from one shot experiment but were successfully reproduced in two experimental campaigns led two years apart, as discussed in Fig. 1.

In these experiments, relevant for fusion, nonlinear kinetic effects are clearly at play. Moreover, nonlinear wave couplings are mostly limited to SRS, which considerably reduces the uncertainties related to the modeling of laser-plasma interaction. Nevertheless, we cannot guarantee that such effects as laser filamentation does not have an impact on Raman reflectivity nor that the electron and ion temperatures and densities are perfectly estimated by TROLL. Although an in-depth study of these issues is way beyond the scope of our work, we do discuss them in this Letter based on the results shown in Figs. 2 and 4. This will greatly help clarifying PIEM's ability to correctly model SRS for the experiment at the Ligne d'Intégration Laser considered in this Letter.

PIEM. PIEM works as a nonlinear gain model along rays with curvilinear abscissa, *s*. The main difference with previously published gain models [11,12] lies in the account of nonlinear kinetic effects, in Eq. (3), in order to derive the electron plasma wave (EPW) amplitude. More precisely, PIEM equations for SRS are

$$\partial_s A_l^2 = -\frac{ek_p \operatorname{Re}(E_p)}{m\sqrt{\omega_b\omega_l}\sqrt{v_{g_l}v_{g_b}}}\sqrt{\frac{\zeta_b}{\zeta_l}}A_l[A_b + A_{b_f}], \quad (1)$$

$$\partial_s A_b^2 = -\frac{ek_p \operatorname{Re}(E_p)}{m\sqrt{\omega_b\omega_l}\sqrt{v_{g_l}v_{g_b}}}\sqrt{\frac{\zeta_l}{\zeta_b}}A_lA_b, \quad (2)$$

$$E_p = \frac{\Gamma_p\sqrt{\omega_b\omega_l}}{\gamma + v_p - i\delta\omega}\sqrt{\frac{v_{g_l}}{v_{g_b}}}\sqrt{\zeta_l\zeta_b}E_{l_0}^2A_l[A_b + A_{b_f}], \quad (3)$$
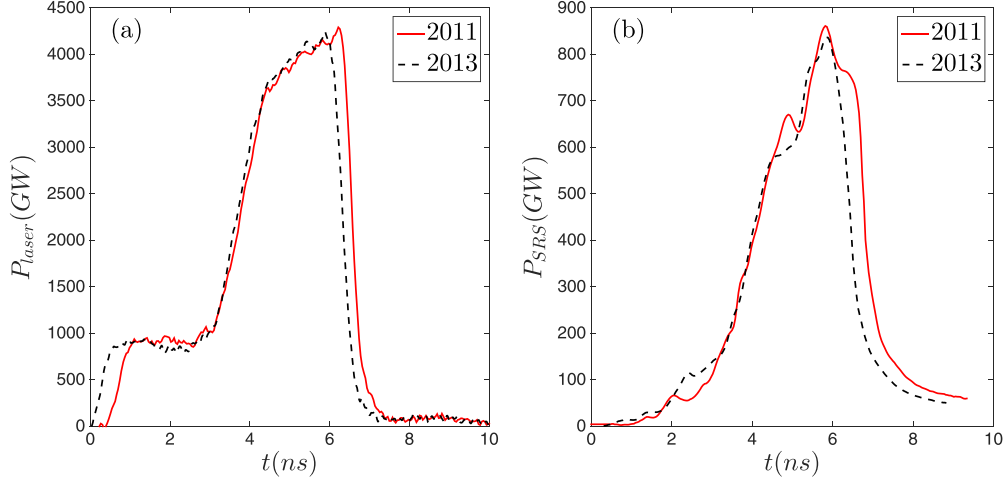
*didier.benisti@cea.fr

FIG. 1. (a) Incident laser power used in the 2011 campaign (red solid line) and in the 2013 campaign (black dashed line). (b) SRS reflected power measured in the 2011 campaign (red solid line) and in the 2013 campaign (black dashed line). The reflectivity decreases later in the 2011 campaign due to a later decrease of the incident power.

where $-e$ is the electron charge and m its mass, and where the subscripts l,b,p are respectively for the laser, backscattered, and plasma waves. For each wave, we use ω to denote the frequency, k for the wave number, and E for the amplitude. In Eqs. (1)–(3), $v_{g_{l,b}} = |k_{l,b}| c^2/\omega_{l,b}$, where c is the speed of light in vacuum. $\zeta_l = \int_0^s e^{-v_l/v_{g_l}} dx$ and $\zeta_b = \int_s^{s_{\max}} e^{-v_b/v_{g_b}} dx$, where $v_{l,b}$ are the rates of power absorption due to inverse bremsstrahlung. They are derived by accounting for the so-called Langdon effect, as described in Ref. [13]. Moreover, $s = 0$, respectively $s = s_{\max}$, is the coordinate when the ray has entered, respectively exited, the plasma. In Eq. (3), E_{l_0} would be the laser wave amplitude absent of SRS and damping. Then, the electric field amplitudes, E_l and E_b, for the laser and backscattered waves are related to A_l and A_b by $E_l = \sqrt{\zeta_l \omega_l} A_l E_{l_0}$, $E_b = \sqrt{\zeta_b \omega_b v_{g_b}/v_{g_l}} A_b E_{l_0}$. We also introduce E_{b_f} as the amplitude of the fluctuations at frequencies

close to ω_b, which seed SRS. It is related to A_{b_f} by $E_{b_f} = \sqrt{\zeta_b \omega_b v_{g_b}/v_{g_l}} A_{b_f} E_{l_0}$. We did not try to make an accurate estimate for E_{b_f} and we simply assumed $E_{b_f} = \eta E_{l_0}$.

The results shown in this Letter correspond to $\eta = 10^{-5}$ but we varied η from 10^{-7} to 10^{-3} without finding any significant change in the reflectivity. This is because the reflectivity is strongly limited by nonlinear saturation mechanisms, such as pump depletion, wave breaking [9], and Langmuir decay instability (LDI) [14]. Note that, in the simulation results obtained with our three-dimensional (3D) envelope code BRAMA [15], we also obtained a good agreement with the experimental measurements when $\eta = 10^{-5}$. Moreover, when the SRS reflectivity was more than about 1%, we also found that it was essentially independent of our choice for η. A more accurate modeling of the noise level might be necessary to predict very small reflectivities, significantly less than 1%. However, this is

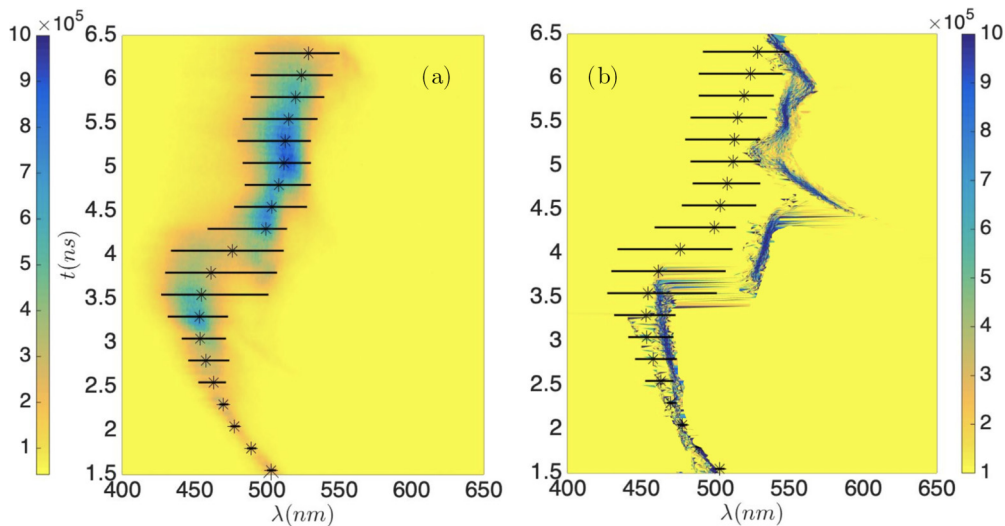FIG. 2. SRS-reflected spectrum (a) as measured experimentally and (b) as predicted by PIEM in arbitrary units. In both figures, the black stars and the horizontal lines indicate, respectively, the wavelengths at maximum and the widths of the experimental spectrum. The PIEM spectrum in (a) was designed so as to assume time-independent maxima, which is in contrast with the experimental spectrum in (b).
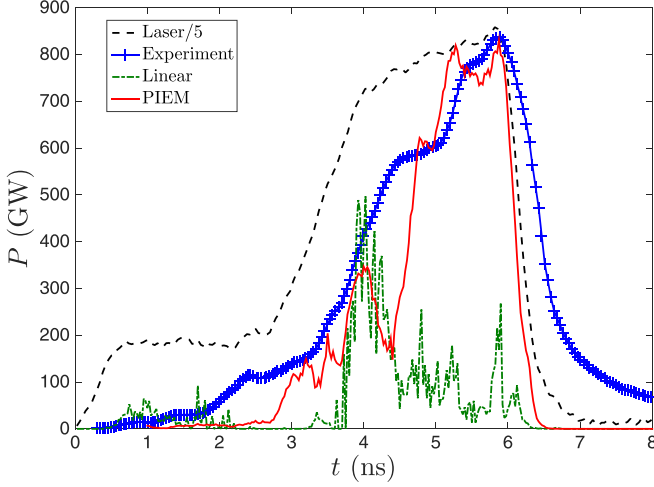
FIG. 3. SRS reflected power as measured experimentally (blue curve with pluses), as predicted by PIEM (red solid line), and by a linear model (green dashed-dotted line). The black dashed line is the incident laser power divided by 5.

beyond the scope of our work because PIEM does not aim to estimate very accurately SRS reflectivity when it is negligible.

Except for the use of the variables A_l and A_b, Eqs. (1) and (2) for the electromagnetic waves are essentially the same as those used in Refs. [11,12]. A_b^2 is proportional to the number of photons created by Raman backscattering, so that $A_b(s = s_{\max}) = 0$, and A_l^2 is proportional to the number of laser photons and is normalized so that $A_l(s = 0) = 1$. Then, Eqs. (1) and (2) simply express how the number of laser and backscattered photons vary along a ray. In particular, when there is no absorption nor spontaneous emission, i.e., when $\zeta_l = \zeta_s = 1$ and when $A_{b_f} = 0$, these equations lead to $(A_l^2 - A_b^2) = $ const. This simply expresses the fact that the destruction of laser photons by SRS leads to the creation of the same number of backscattered photons.

In Eq. (3), $\nu_p = (1 - Y_{\mathrm{NL}})\nu_L$, where ν_L is the Landau damping rate [16]. As for Y_{NL}, it is the fraction of electrons
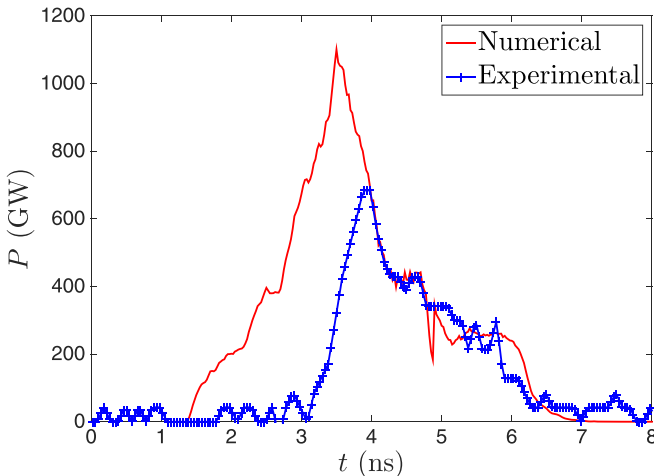

FIG. 4. Transmitted power as derived numerically (red solid line) and as measured experimentally (blue solid line with pluses).

which respond nonlinearly to the EPW. It is derived by using the result, shown in Ref. [17], that an electron responds non-linearly to the EPW once it has nearly completed one trapped orbit in the wave trough. Then, as shown in Ref. [8], in a three-dimensional geometry and for a Maxwellian plasma,

$$Y_{\mathrm{NL}} = 1 - \exp\left(-\omega_B^2 l_\perp^2/50 v_{\mathrm{th}}^2\right), \qquad (4)$$

where v_{th} is the electron thermal speed, $\omega_B = \sqrt{2ek_p|E_p|/m}$ is the so-called bounce frequency, and $l_\perp$ is a typical transverse gradient length for E_p. An exact expression for Y_{NL} would require an exact estimate of $l_\perp$. However, it cannot be very different from the choice made in this Letter, $l_\perp = \lambda_l f_\#$, where λ_l is the laser wavelength and $f_\#$ the overall aperture of the focusing system. Now, ω_B^2 varies very quickly with the laser intensity so that a little change in $l_\perp$ would entail a very small change in the threshold intensities leading to $Y_{\mathrm{NL}} \approx 1$, and would have an insignificant impact on our results. Hence, no fine tuning is necessary for $l_\perp$, which is not to be considered as a free parameter of our model.

In Eq. (3),

$$\delta\omega = (1 + \chi)/\partial_\omega \chi, \qquad (5)$$

where $\chi(k, \omega)$ may be viewed as a nonlinear electron suscep-tibility, derived in Refs. [8,17]. It reads

$$\chi = (1 - Y_{\mathrm{NL}})\chi_{\mathrm{lin}} + Y_{\mathrm{NL}}\chi_a, \qquad (6)$$

where χ_{lin} is the linear electron susceptibility whose expres-sion may be found in Ref. [18], and where χ_a is the adiabatic nonlinear susceptibility whose expression may be found in Refs. [9,10,17]. Then, in Eq. (3), $\Gamma_p = ek_p/m\omega_l\omega_b\partial_\omega\chi$, and

$$\gamma = \sqrt{\gamma_0^2 + \nu_p^2} - \nu_p, \qquad (7)$$

where $\gamma_0 = k_p v_{\mathrm{osc}}/\sqrt{2\omega_b\partial_\omega\chi_{\mathrm{lin}}}$ with $v_{\mathrm{osc}} = eE_{l_0}/m\omega_l$. Equa-tion (7) for γ is an estimate of the EPW growth rate which proved to yield very accurate results, in Ref. [10] as regards the nonlinear EPW growth, and in Ref. [19] as regards the derivation of the EPW nonlinear frequency shift. If we had used $\gamma = E_p^{-1}(\partial_t + v_{g_p}\partial_x)E_p$, with $v_{g_p} = -\partial_k\chi/\partial_\omega\chi$, Eq. (3) would just have been the envelope equation,

$$\partial_\omega\chi[\partial_t + v_{g_p}\partial_s + \nu_p]E_p - i(1 + \chi)E_p = \Gamma_p\partial_\omega\chi E_l E_b^{\mathrm{tot}}. \quad (8)$$

Equation (8) has been derived in Ref. [17] and its accuracy has been directly tested against Vlasov simulations in Ref. [20]. It has also been used in our envelope code BRAMA [21], whose accuracy has been tested in Ref. [22] against Vlasov simu-lations, and in Ref. [15] against the experimental results of Ref. [23]. Using Eq. (7) for γ instead of solving the envelope equation (8) makes PIEM an effective gain model.

In Eqs. (5) and (8), we use $\chi(k = k_l - k_b, \omega = \omega_l - \omega_b)$. Then, the term $-i\delta\omega$ in the denominator of the right-hand side of Eq. (3) accounts for SRS detuning due to the plasma inhomogeneity and to the nonlinear frequency shift. They may either compensate and even lead to autoresonance [24] or add up and saturate SRS. Moreover, when solving Eq. (3), we account for saturation due to LDI and wave breaking. To do so, we enforce the condition $E_p < E_{\max}$, where $E_{\max}$ is the minimum between the limit imposed by LDI, as derived in

Ref. [14], and that imposed by wave breaking, as derived in Ref. [10].

As regards the amplitude, E_{l_0}, for the laser electric field absent of SRS, we cannot rely on the estimate E_{l_g} of our rad-hydro code, because it stems from geometrical optics. In order to account for optical smoothing used in ICF [25], which leads to a speckle pattern, we use $E_{l_0}^2(s) = \alpha_{\mathrm{liss}}(s) E_{l_g}^2(s)$, where $\alpha_{\mathrm{liss}}(s) \equiv \sum_i \alpha_i(s - \sigma_i)$. Here, α_i is a bell-shaped function whose total width at half maximum is of the order of the longitudinal size, $l_\parallel$, of a speckle. We chose $\alpha_i(s) = \alpha_{0_i} \sin_c^2[\pi(s/l_\parallel)]$, where α_{0_i} is an exponential random variable. Moreover, we impose the averaged value of α_{liss} to be unity along each ray. As for the σ_i's, there are separated by $2l_\parallel$ and are time independent, so that we do not account for smoothing by spectral dispersion (SSD). This would impose too small time steps in our rad-hydro simulation, while SRS usually grows too quickly to be directly sensitive to SSD. As regards $l_\parallel$, we chose $l_\parallel = 7\lambda_l f_\#^2$ but we could have used a slightly different value. However, a small change in $l_\parallel$ would entail, at most, a very small shift in the intensity dependence of the reflectivity. Hence, $l_\parallel$ is not to be considered as a free parameter of our model.

Along each ray, Eqs. (1)–(3) are solved for one single value of ω_b. It is derived every $N_{w_b^*}$ time steps as the frequency yielding the largest Raman reflectivity. The chosen value for ω_b fulfills the three-wave resonance conditions at a given abscissa, s^*. Then, at s^*, we generate a backscattered wave that carries a number of photons, N_b, derived from the resolution of Eq. (2). This wave propagates along its own ray and deposits its energy in the plasma by inverse bremsstrahlung. Moreover, at $s = s^*$, the laser wave is depleted by N_b photons. Hence, we allow for the SRS feedback on the plasma hydrodynamics.

When solving Eqs. (1) and (2), we assume that the ray trajectories are identical for the laser and backscattered waves, which is clearly valid when the plasma is nearly uniform. When the plasma is inhomogeneous, SRS is only effective within the narrow space region where the resonance conditions $k_l - k_b = k_p$ and $\omega_l - \omega_b = \omega_p$ are fulfilled. Within this region the laser and backscattered ray trajectories are nearly the same. Finally, note that Eqs. (1) and (2) are only valid when the wave amplitudes do not explicitly depend on time. Hence, we miss the distinction between a convective and an absolute linear instability [26,27]. However, in this Letter, we address the nonlinear regime of SRS and we mainly want to estimate the maximum amplitude reached by the backscattered wave, which follows from the limits imposed on the EPW amplitude by nonlinear saturation mechanisms.

Numerical resolution. Equation (3) for E_p is solved by bisection [28], with $0 \leqslant E_p \leqslant E_{\max}$, where $E_{\max}$ is the minimum between the limit imposed by LDI [14] or by wave breaking [10]. In order to significantly speed up PIEM, we derive $\delta\omega$ from stored values obtained for a large range of electron densities and temperatures, and of EPW amplitudes. Eqs. (1) and (2) are solved by making use of a fourth-order Runge-Kutta method [28], with the space step $\delta s \approx 5$ μm. These equations are solved from $s = 0$ to $s = s_{\max}$ for a given value of $A_b(0)$. Now, the value of $A_b(0)$ that yields our estimate for the reflected power is found by bisection. Knowing that $0 \leqslant A_b(0) \leqslant \sqrt{\omega_b/\omega_l} \zeta_b(0)$ we solve Eqs. (1)–(3) until

we find, using the bisection method, the value $A_b(0)$ that yields $A_b(s_{\max}) \approx 0$. As for the plasma hydrodynamics, it was computed by making use of a two-dimensional axisymmetric TROLL simulation. The time step used for the simulation was $\delta t = 0.5$ ps. Moreover, we used $N_{w_b^*} = 15$ which let us estimate ω_b every 7.5 ps, which is much less than the time needed for the electron density and temperature to vary significantly (we also tried $N_{w_b^*} = 10$ and found essentially the same results). Note that, because PIEM calculates SRS along rays, its performance should not be very sensitive to dimensionality. In our simulation, we used $33^2 = 1089$ rays.

Comparisons against experimental results. In this Letter, we do not simply compare PIEM against one experimental measurement, but we carefully discuss PIEM's ability to make accurate predictions for one experimental configuration relevant to laser fusion. It corresponds to the experiments detailed in Ref. [29], performed in two similar campaigns at the Ligne d'Intégration Laser (LIL) in 2011 and 2013, and leading to very similar reflectivities as shown in Fig. 1. The laser system of the LIL facility consisted of four square beamlets, put together into a quad, with a total energy close to 15.7 kJ. The temporal pulse shape, illustrated in Figs. 1(a) and 3, consisted of two plateaus, of about 3 ns each. The power in the first plateau was close to 1 TW (with a space-averaged intensity close to $2 \times 10^{14} \mathrm{W/cm^2}$), and the power in the second plateau was about 4–4.5 TW (which corresponds to a space-averaged intensity of about $8–9 \times 10^{14} \mathrm{W/cm^2}$). The quad was optically smoothed with kinoform phase plates and the pilot incorporated two phase modulators, one at 2 GHz and one at 14 GHz. The quad was sent into a cylindrical hohlraum, 4 mm long and 1.4 mm diameter, filled with 1 atm neo-pentane gas. The hohlraum was closed by two thin polymide windows which exploded under the action of the quad. Hence, this was an open configuration.

Let us first compare the wavelengths of the reflected light as measured experimentally against those predicted by PIEM. There are very similar between $t = 1$ns and $t \approx 3.75$ns and between $t \approx 5$ns and $t = 6.5$ns, except that the PIEM spectrum is thinner because, in PIEM, we only retain one wavelength per ray. At $t \approx 3.75$ns, there are two maxima in the experimental and numerical spectra, which indicates that SRS is generated in plasma regions with different electron densities. Actually, when the laser quad enters the hohlraum, the plasma is first expelled from the propagation axis, and bounces against the hohlraum wall before coming back towards the axis when $t \approx 3.75$ns. Hence, there is plasma mixing, which TROLL does not simulate very accurately. This may be one reason for the discrepancies in the spectra between 4 and 5 ns.

As regards the SRS reflected power, Fig. 3 shows that PIEM predictions are in good agreement with the experimental measurements between $t = 3$ns and $t = 6$ns, except when $t \approx 4.5$ns. As may be seen in Fig. 2, the agreement between the experimental and numerical spectra is worst precisely at $t \approx 4.5$ns. More generally, between $t = 3$ns and $t = 6$ns, there is a close correlation between the agreement on the reflectivity and the agreement on the spectra. This seems to indicate that, within this time interval, PIEM accuracy is mainly limited by TROLL's ability to correctly simulate the plasma hydrodynamics.
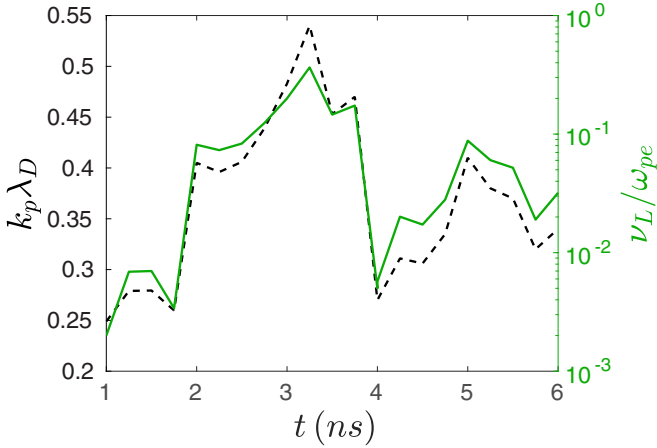
FIG. 5. Time evolution of $k_p\lambda_D$ (black dashed line) and of ν_L/ω_{pe} (green solid line) as calculated by PIEM.

Now, when $t < 3$ns, PIEM predictions for the SRS reflectivity strongly underestimate the experimental data. Figure 4 also shows that, before 3–4ns, our numerical predictions for the transmitted power strongly overestimate the experimental measurements. This overestimate is very unlikely to be related to stimulated Raman scattering since the SRS reflectivity is very low when $t \leqslant 3$ns. Moreover, in Fig. 4, we account for the difference between the numerical and experimental values of the reflectivity in order to estimate the transmission. Namely, we plot $T = T_{\mathrm{PIEM}} + R_{\mathrm{PIEM}} - R_{\mathrm{expt}}$, where T_{PIEM} and R_{PIEM} are, respectively, the transmitted and reflected powers as predicted by PIEM, and R_{expt} is the SRS reflected power as measured experimentally. The discrepancies illustrated in Fig. 4 would rather indicate that, before 3–4ns, some physical effects, different from SRS, are not correctly modeled in our rad-hydro simulation. This may be the heat flux, leading to a poor estimate of the plasma temperatures and of the absorption of the incident laser energy. This may also be laser filamentation, which may prevent the beams from exiting the hohlraum and which we do not account for in our TROLL simulation. Consequently, it is difficult to draw any conclusion on PIEM accuracy from the comparisons against the experimental results before 3 ns.

In Fig. 3 we also plot the predictions for the SRS reflectivity as derived from the linear model described in Ref. [11], which has been recently implemented in TROLL. This model systematically underestimates both the PIEM predictions and the experimental measurements, except when $t \approx 4$ns. Now, from the spectrum of Fig. 2(b), we know the electron density n_e where SRS mainly grows. Moreover, in our simulation, we

know where most of the backscattered rays come from, which allows us to derive the electron temperature T_e. From n_e and T_e we can derive the value of $k_p\lambda_D$ ($\lambda_D = v_{\mathrm{th}}/\omega_{pe}$ being the Debye length) and of the Landau damping rate ν_L for the EPW resulting from SRS.

As may be seen in Fig. 5, ν_L assumes a marked minimum when $t \approx 4$ns. It is several times smaller than γ_0, so that its nonlinear decrease has a very moderate impact on SRS. This is in contrast with the situation at earlier and later times when ν_L assumes much larger values, respectively, because the density is smaller or because the temperature is larger. Actually, as shown in Fig. 3, ν_L grows so quickly after $t \approx 4$ns that the linear reflectivity globally decreases although the laser power raises. This is in contrast with PIEM's prediction for the reflectivity, which globally increases after $t \approx 4$ns, in agreement with the experimental results. This shows PIEM's ability to correctly account for the nonlinear reduction of the EPW damping rate, and more generally for the impact of nonlinear kinetic effects on SRS. Comparisons against linear results are clear evidence of kinetic inflation [30] and of PIEM's ability to allow for it.

Conclusion. In this Letter, we introduced the PIEM model, able to correctly predict the SRS reflected power measured on LIL experiments when nonlinear kinetic effects were clearly at play. This does not mean that we are able to make predictive ICF simulations for all possible situations. We do not claim that PIEM is perfect and complete. In the near future, we want to extend our theory for EPWs to ion waves in order to derive a nonlinear kinetic modeling for stimulated Brillouin scattering and crossed beam energy transfer that would be included in PIEM, in addition to SRS. We also want to allow for the production of hot electrons by SRS after the EPW breaks up. So far, since we do not have a theory for the distribution of such electrons, we do not account for the deposition of their energy in the plasma. Several issues, related to laser beam propagation, plasma hydrodynamics, or laser power absorption, may also need to be more accurately accounted for in TROLL. More comparisons against experimental measurements, possibly from other groups using data from other facilities, would be useful, and this is one motivation to have this work published. We do believe that PIEM opens the path to predictive simulations by successfully addressing one important issue, long thought as a particularly difficult one. It lets a radiation hydrodynamics code correctly estimate nonlinear kinetic effects.

[1] W. Kruer, *The Physics of Laser Plasma Interactions* (Addison-Wesley, Redwood City, CA, 1988).

[2] N. B. Meezan, L. J. Atherton, D. A. Callahan, E. L. Dewald, S. Dixit, E. G. Dzenitis, M. J. Edwards, C. A. Haynam, D. E. Hinkel, O. S. Jones *et al.*, Phys. Plasmas **17**, 056304 (2010); N. B. Meezan, L. J. Atherton, E. J. Bond, D. A. Callahan, E. L. Dewald, S. Dixit, E. G. Dzenitis, M. J. Edwards, C. A. Haynam, D. E. Hinkel *et al.*, *ibid.* **17**, 109901(E) (2010).

[3] H. Abu-Shawareb, R. Acree, P. Adams, J. Adams, B. Addis, R. Aden, P. Adrian, B. B. Afeyan, M. Aggleton, L. Aghaian *et al.*, Phys. Rev. Lett. **129**, 075001 (2022).

[4] D. J. Stark, L. Yin, T. B. Nguyen, G. Chen, L. Chacon, B. M. Haines, and L. Green, Phys. Plasmas **30**, 042714 (2023).

[5] A. Colaïtis, G. Duchateau, X. Ribeyre, Y. Maheut, G. Boutoux, L. Antonelli, P. Nicolai, D. Batani, and V. Tikhonchuk, Phys. Rev. E **92**, 041101(R) (2015).

[6] D. J. Strozzi, D. S. Bailey, P. Michel, L. Divol, S. M. Sepke, G. D. Kerbel, C. A. Thomas, J. E. Ralph, J. D. Moody, and M. B. Schneider, Phys. Rev. Lett. **118**, 025002 (2017).

[7] E. Lefebvre, S. Bernard, C. Esnault, P. Gauthier, A. Grisollet, P. Hoch, L. Jacquet, G. Kluth, S. Laffite, S. Liberatore *et al.*, Nucl. Fusion **59**, 032010 (2019).

[8] D. Bénisti, Plasma Phys. Control. Fusion **60**, 014040 (2018).

[9] M. Tacu and D. Bénisiti, Phys. Plasmas **29**, 052108 (2022).

[10] M. Tacu and D. Bénisiti, Phys. Plasmas **29**, 052109 (2022).

[11] A. Debayle, C. Ruyer, O. Morice, P.-E. Masson-Laborde, P. Loiseau, and D. Benisti, Phys. Plasmas **26**, 092705 (2019).

[12] D. J. Strozzi, E. A. Williams, D. E. Hinkel, D. H. Froula, R. A. London, and D. A. Callahan, Phys. Plasmas **15**, 102703 (2008).

[13] A. B. Langdon, Phys. Rev. Lett. **44**, 575 (1980).

[14] T. Kolber, W. Rozmus, and V. T. Tikhonchuk, Phys. Fluids B **5**, 138 (1993).

[15] D. Bénisti, O. Morice, L. Gremillet, A. Friou, and E. Lefebvre, Phys. Plasmas **19**, 056301 (2012).

[16] L. D. Landau, J. Phys. (Moscow) **10**, 25 (1946).

[17] D. Bénisti and L. Gremillet, Phys. Plasmas **14**, 042304 (2007).

[18] D. Bénisti, Phys. Plasmas **22**, 072106 (2015).

[19] D. Bénisti, D. J. Strozzi, and L. Gremillet, Phys. Plasmas **15**, 030701 (2008).

[20] D. Bénisti, D. J. Strozzi, L. Gremillet, and O. Morice, Phys. Rev. Lett. **103**, 155002 (2009).

[21] D. Bénisti, O. Morice, L. Gremillet, E. Siminos, and D. J. Strozzi, Phys. Plasmas **17**, 102311 (2010).

[22] D. Bénisti, O. Morice, L. Gremillet, E. Siminos, and D. J. Strozzi, Phys. Rev. Lett. **105**, 015001 (2010).

[23] D. S. Montgomery, J. A. Cobble, J. C. Fernàndez, R. J. Focia, R. P. Johnson, N. Renard-Le Galloudec, H. A. Rose, and D. A. Russell, Phys. Plasmas **9**, 2311 (2002).

[24] T. Chapman, S. Huller, P. E. Masson-Laborde, A. Heron, D. Pesme, and W. Rozmus, Phys. Rev. Lett. **108**, 145003 (2012); L. Friedland, *ibid.* **69**, 1749 (1992).

[25] J. C. Garnier, C. Gouedard, L. Videau, and A. Migus, Proc. SPIE **3047**, 260 (1997).

[26] R. Q. Twiss, Proc. Phys. Soc. B **64**, 654 (1951).

[27] A. Bers, in *Handbook of Plasma Physics*, edited by M. N. Rosenbluth and R. Z. Sagdeev (North-Holland, Amsterdam 1983), Vol. 1, Chap. 3.2; R. Z. Briggs, *Electron-Stream Interaction with Plasmas* (MIT Press, Cambridge, MA, 1964).

[28] W. H. Press, S. A. Teukolsky, W. T. Vetterling, and B. P. Flannery, *Numerical Recipes* (Cambridge University Press, Cambridge, UK, 2007).

[29] C. Rousseaux, G. Huser, P. Loiseau, M. Casanova, E. Alozy, B. Villette, R. Wrobel, O. Henry, and D. Raffestin, Phys. Plasmas **22**, 022706 (2015).

[30] H. X. Vu, D. F. Dubois, and B. Bezzerides, Phys. Plasmas **14**, 012702 (2007).